Dalton Transactions

Platin-C Nanoparticles: A Recipe for the Delivery of Curcumin-Cisplatin Combination Chemotherapeutics to Mitochondria

Journal:	*Dalton Transactions*
Manuscript ID	DT-ART-09-2022-003149.R1
Article Type:	Paper
Date Submitted by the Author:	29-Dec-2022
Complete List of Authors:	Banik, Bhabatosh; Gauhati University, Department of Chemistry Ashokan, Akash; University of Miami School of Medicine, Biochemistry and Molecular Biology Choi, Joshua ; University of Georgia Franklin College of Arts and Sciences Surnar, Bapurao; University of Miami School of Medicine, Biochemistry and Molecular Biology Dhar, Shanta; University of Miami School of Medicine, Biochemistry and Molecular Biology

Platin-*C* Nanoparticles: A Recipe for the Delivery of Curcumin-Cisplatin Combination Chemotherapeutics to Mitochondria

Bhabatosh Banik*,[1,2,3,4], Akash Ashokan,[1,2] Joshua H. Choi[3], Bapurao Surnar,[1,2] and Shanta Dhar*,[1,2,3,5]

[1]NanoTherapeutics Research Laboratory, Department of Biochemistry and Molecular Biology, University of Miami Miller School of Medicine, Miami, FL 33136, USA

[2]Sylvester Comprehensive Cancer Center, Miller School of Medicine, University of Miami, Miami, FL 33136

[3]Nano Therapeutics Research Laboratory, Department of Chemistry, University of Georgia, Athens, GA 30602

[4]Department of Chemistry, Cotton University, Panbazar, Guwahati-781001, Assam, India

[5]Department of Chemistry, University of Miami, Coral Gables, FL 33146, USA

*** Correspondence:**
Corresponding Author
bhabatosh.banik@cottonuniversity.ac.in
shantadhar@med.miami.edu

Keywords: Cisplatin, Curcumin, Cisplatin-resistance, Combination-therapeutics, Mitochondria-targeted, Nano-formulation

Abstract: The success story of cisplatin spans over six decades now and yet it continues to be the key player in most chemotherapeutic regimens. Numerous efforts have been made to improve its efficacy, address its shortcomings, and overcome drug resistance. One such strategy is to develop new platinum(IV)-based prodrugs with functionally active ligands to deliver combination therapeutics. This strategy not only enables the drug candidate to access multiple drug targets but also enhances kinetic inertness of platinum complexes and thereby ensures greater accumulation of active drug at the target site. We report the synthesis of Platin-*C*, a platinum(IV) based cisplatin prodrug tethered to the active component of ancient herbal medicine, curcumin, as one of the axial ligands. This combination complex showed improved chemotherapeutic efficacy in cisplatin resistant A2780/CP-70 cell lines when compared to the individual components. An amine-terminated biodegradable polymer was suitably functionalized with triphenylphosphonium (TPP) cation to obtain mitochondria-directed drug delivery platform. Quantification of Platin-*C* loading into these NPs using complementary techniques employing curcumin optical properties in high-performance liquid chromatography and platinum-based inductively coupled plasma mass spectrometry evidenced efficacious payload incorporation to result functional activities of both the components. Stability studies for a period of one week indicated that the NPs remain stable enabling substantial loading and controlled release of the prodrug. The targeted nanoparticle (NP) platform was utilized to deliver Platin-*C* primarily in the mitochondrial network of cancer cells as monitored using confocal microscopy employing the green fluorescence of the curcumin pendant. Our studies showed that amine terminated NPs were relatively less efficient in their ability to target mitochondria despite being positively charged. This re-validated the importance of lipophilic positively charged TPP surface functionalities to successfully target cellular

mitochondrion. We validated the capabilities of Platin-*C* and its mitochondria-targeted nanoparticles towards inflicting mitochondria-directed activity in cisplatin-sensitive and cisplatin-resistant cell lines. Furthermore, our studies also demonstrated the effectiveness of Platin-C incorporated targeted NPs to attenuate cellular inflammatory markers by utilizing curcumin component. This study advances our understandings of cisplatin prodrug approach to combine chemotherapeutic and inflammatory effects in accessing combinatory pathways.

Introduction

Even after 65 years of its discovery, Cis-diamminedichloridoplatinum(II), or cisplatin is still one of the most prescribed anticancer drugs available for the treatment of varied solid tumors.[1-4] Despite the great success in treating cancer, the efficiency of cisplatin is compromised by its induction of several side effects and acquired resistance to its effectiveness [5-7]. Inflammation, on the other hand, is closely related to tumorigenesis.[8-10] Chronic inflammation plays a significant role in approximately 20% of human cancer.[11] The inflammatory genes and cytokines associated with tumors contribute to the formation of immunosuppressive microenvironment conducive for its growth and progression. Moreover, deletion or inhibition of inflammatory cytokines prevents tumor development. Nuclear factor kappa B (NF-κB) is one of the inflammatory genes that is a central regulator of the inflammatory response.[12] Activation of NF-κB promotes cell proliferation while down regulation presents the opposite effect; thus NF-κB is one of major factor in tumorigenesis.[13-15] Curcumin, a major component of the spice, turmeric, is an emissive compound[16-18] that exhibits anti-cancer,[19-21] anti-inflammatory,[22-24] and anti-oxidative[25,26] properties. Specifically, it plays a critical role in controlling the NF-κB signaling pathway by inhibiting phosphorylation of the inhibitor of kappa B, thus causing down regulation of NF-κB [27,28]. It also acts as a radical oxygen species scavenger *via* H-atom donation and electron transfer, thus exhibiting anti-oxidative property.[29] Although it exhibits multiple functions, its efficacy in preclinical and clinical studies is limited because of its poor water solubility and its low bioavailability that is a result of its short biological half-life.[30,31] To circumvent these problems, delivery vehicles have been used to deliver curcumin to the target rapidly and accurately.[32,33] A combination of curcumin and cisplatin can be an lucrative strategy for managing cancer.[34-36] Administration of free-drug formulations may pose hurdles including definitive exposure of the drugs at the targets of action, differential pharmacokinetic, and biodistribution parameters. These factors, though very difficult to control upon individual administration of the drugs, can however be overcome *via* construction of a single combination prodrug constituting the drugs of interest.[37-42] Thus, we envisioned an alternative way to deliver a chemotherapeutic combination of curcumin and cisplatin by fabricating them into a platinum (IV) prodrug that, under the reductive intracellular environment, would give the respective active components. In addition to ascertaining specific stoichiometric composition of the active components, a suitably designed platinum (IV) complex would enhance the circulation lifetime of the prodrug greatly owing to the higher kinetic inertness of such complexes.[2] Our laboratory has made similar efforts in the past to successfully develop combination therapeutic complex of cisplatin and aspirin packaged into a platinum (IV) prodrug called Platin-*A* and demonstrated that it was capable of diminishing chemotherapy associated inflammation.[43-45] With previous experiences along with the associated challenges and opportunities in mind, we blended cisplatin and curcumin into a platinum (IV) complex, Platin-*C*, which can be reduced to yield the constituent active components and direct those to their respective biological actions.

Another added dimension that can provide tremendous additional advantage towards the activity of the prodrug is to target the mitochondria of tumor.[42,46-49] We have designed triphenyl phosphonium (TPP) cation functionalized polymeric nanoparticles (NPs) that, by virtue of its lipophilic delocalized positive charge, is selectively taken up by mitochondria.[50-55] Surface modification of the FDA-approved

polymer, poly(lactic-*co*-glycolic acid)-block-poly(ethylene glycol) block copolymer (PLGA-*b*-PEG), with TPP cation is a promising method of delivering payloads into mitochondria.[53-55]

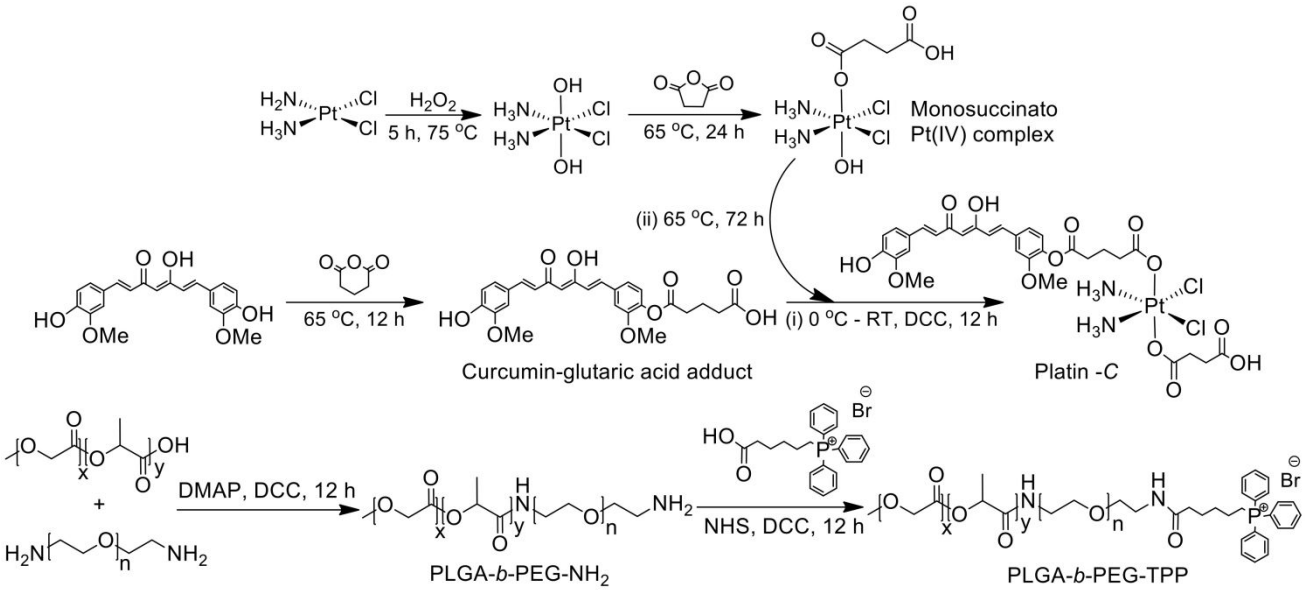

Scheme 1. Scheme depicting the strategy adopted for synthesis of the complexes, ligands and polymers.

Results and Discussion

Synthesis and Characterization of Platin-C

As described above, Platin-*C* is a Pt(IV) complex tethered to curcumin via glutaric acid linker at one of the axial coordination sites. Curcumin was reacted with glutaric anhydride to yield the curcumin-glutaric acid adduct, which was then treated with dicylohexylcarbodiimide (DCC) in presence of catalytic amounts of 4-dimethylaminopyridine (DMAP) to produce the corresponding anhydride. On the other hand, cisplatin was oxidized using hydrogen peroxide following the well-known literature procedure to generate *cis,cis,trans*-diamminedichlorodihydroxoplatinum(IV). It was then allowed to react with an equivalent amount of succinic anhydride to generate *cis,cis,trans,*-diamminedichlorohydroxosuccinatoplatinum(IV). In the final step, this *cis,cis,trans,*-diamminedichlorohydroxosuccinatoplatinum(IV) was further reacted with the anhydride of curcumin-glutaric acid adduct to yield the final product *i.e.*, Platin-*C*. While the curcumin-glutaric acid adduct was characterized using ^{1}H and ^{13}C NMR (Supp. Fig. 1 and 2), its anhydride was prepared freshly and used for subsequent reactions without any purification. *cis,cis,trans*-diamminedichlorodihydroxoplatinum(IV) and *cis,cis,trans,*-diamminedichlorohydroxosuccinatoplatinum(IV) were synthesized using previously standardized protocol form our laboratory[56] and the characteristic peaks in the ^{1}H NMR spectrum confirmed the composition and purity of the desired complexes. The final product, Platin-*C* was characterized using ^{1}H NMR, gCOSY, ^{13}C NMR, ^{195}Pt NMR, and ESI-mass spectrometry techniques (Fig. 1 and Supp. Fig. 3-5). The results suggested that Platin-*C* was produced in analytically pure form. Purity of Platin-*C* was also ascertained by HPLC technique (Supp. Fig. 6). The HPLC chromatogram showed distinctly separate peaks for Platin-*C* and curcumin and the retention time for Platin-*C* was lesser than that of Curcumin indicating an increase in the polarity in the resultant complex. The appearance of a peak at ~1230 ppm in the ^{195}Pt NMR confirmed the presence of Pt in its +4-oxidation state. The peak at 897.3

in mass spectral data also confirmed the formation of Platin-*C*. The isotopic peak patterns reconfirmed the neutral nature of the coordination complex as evidenced from the fact that one m/z unit separates the peaks.

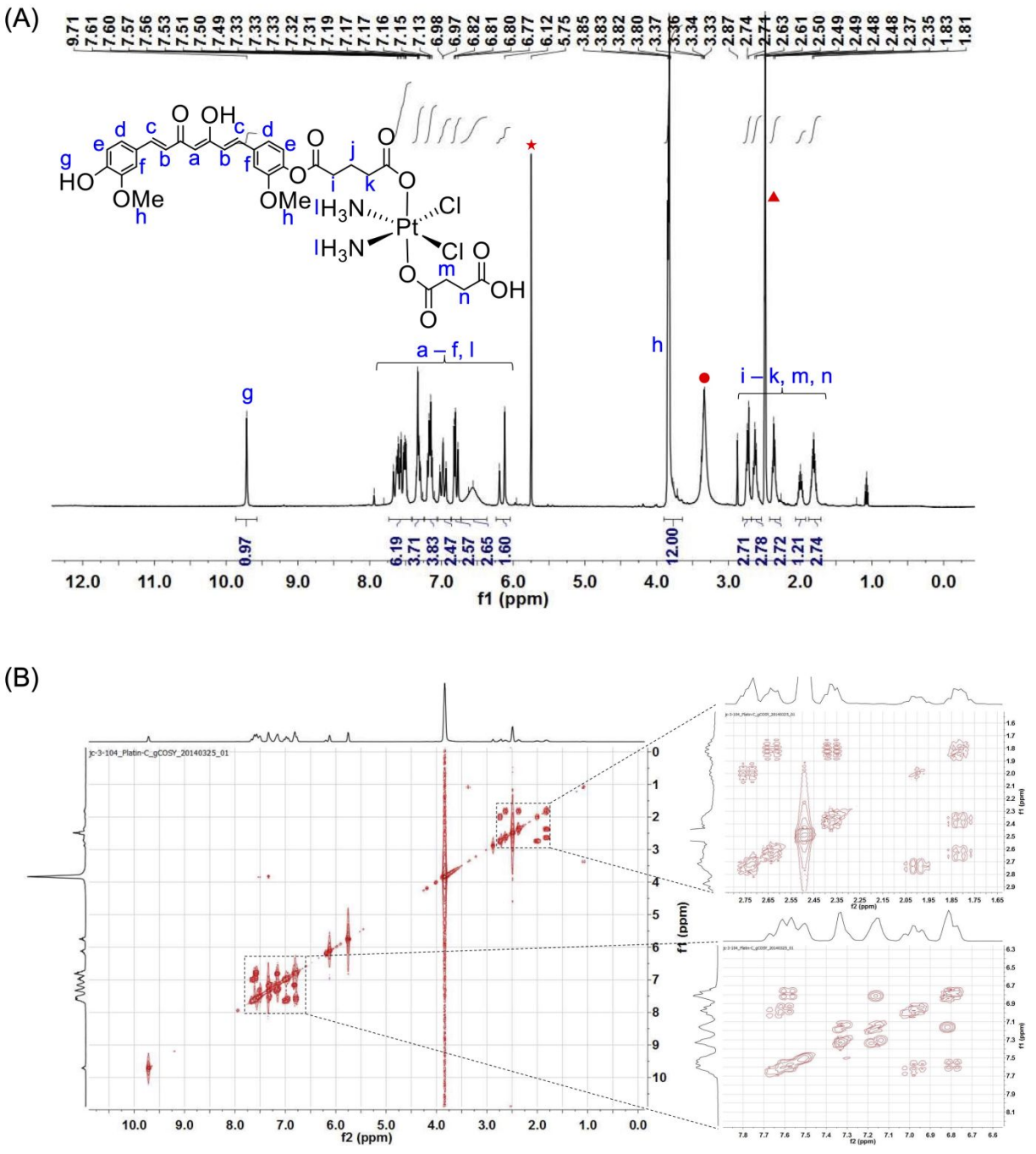

Fig. 1. (A) ^{1}H NMR spectrum of Platin-*C* recorded using a 400 MHz NMR spectrometer. Solvent residual peaks for dichloromethane, water and dimethyl sulphoxide in DMSO-d_6 have been labeled using symbols (in red). (B) gCOSY NMR spectrum of Platin-*C* in DMSO-d_6 recorded using a 400 MHz NMR spectrometer. Individual spectra have also been provided as supporting figures 3 and 4.

Synthesis and Characterization of the Polymers

Another aspect of this work is associated with the synthesis of the non-targeted PLGA-*b*-PEG-NH_2 polymer and the mitochondria-targeted PLGA-*b*-PEG-TPP polymer. Since both these polymers yield nanoparticles with positive zeta potentials, with the help of these polymers we intended to validate the role of lipophilic delocalized positive charge of triphenylphosphonium (TPP) cation in delivering drug cargo preferentially to the mitochondrion of cells. The non-targeted polymer was synthesized employing DCC/DMAP assisted amide coupling between PLGA-COOH and NH_2-PEG-NH_2. Careful control over the stoichiometry and reaction conditions during this reaction afforded formation of the desired polymer rather than conjugation of PLGA at both ends of PEG. This polymer was further functionalized with TPP hexanoic acid to obtain the targeted polymer. Both the polymeric platforms were characterized using ^{1}H NMR, ^{13}C NMR, and gel permeation chromatographic (GPC) techniques (Supp. Fig. 7-11). While NMR ascertained purity of the synthesized polymers, molecular weights and polydispersity indices of the polymers were determined using GPC. The number averaged molecular weights (M_n) and polydisperity indices (PDI) of the non-targeted and targeted polymers as determined GPC using DMF eluent were found to be 21,200 g/mol (PDI = 1.61) and 22,600 g/mol (PDI = 1.81) respectively.

Synthesis and Characterization of the Targeted and Non-targeted Platin-C Nanoparticles

Targeted and non-targeted nanoparticles were loaded with increasing amounts of Platin-*C* using nanoprecipitation technique (Fig. 2A). Dynamic light scattering (DLS) analyses revealed that the NPs were 40-80 nm in diameter. Both NT-NPs and T-NPs had zeta potential of ~40 mV when they are not loaded with Platin-*C* but it drops to ~30 mV for T-NPs and ~20 mV for NT-NPs when they are loaded with the Platin-*C* complex (Fig. 2B and Supplementary Fig. 12 for NT-Platin-*C*-NP). This could be due to the partial neutralization of the positive charges on the polymers by the carboxylate and phenolate groups present on Platin-*C*. Nonetheless, the polymeric nano-constructs were still found to have positive surface charge and the partial decrease in charge could be indicative of successful encapsulation of Platin-*C*. We calculated percent loading and percent encapsulation efficiency (EE) of Platin-*C* in T-NPs by using different percent feed of Platin-*C* with respect to the polymer used in the nanoprecipitation. We utilized this library of NPs to quantify Platin-C in the NPs by using platinum-based inductively coupled plasma mass spectrometry (ICP-MS) (Fig. 2C) and employing curcumin optical properties in high-performance liquid chromatography (Fig. 2D). These data evidenced efficacious payload incorporation to result functional activities of both the components. On careful observation of the size of T-NPs with increasing Platin-*C* concentration, we observed that the size started to increase with loading of 30% or more. So, we anticipated that the sizes of the NPs would go beyond 100 nm for 40% Platin-*C* feed in T-NPs and therefore we carried out all further investigations with NPs having 20% Platin-*C* feed. A 20% feed of Platin-*C* into these NPs resulted in ~7% loading of the complex and this amounts to an encapsulation efficiency of ~30%. This shows the ability of the polymeric platforms to encapsulate Platin-*C* successfully into NP formulations and may therefore prove to be efficient delivery vehicles capable of depositing the drug candidate at the site of action in substantially high concentrations. Percent loading and %EE of Platin-*C* in NT-NPs at percent feed of 20% by HPLC and ICP-MS indicated similar Platin-*C* profile as observed with T-NPs (Fig. 2E). Further, transmission electron microscope (TEM) images of the NPs showed spherical particles with uniform size and shape (Fig. 2F).

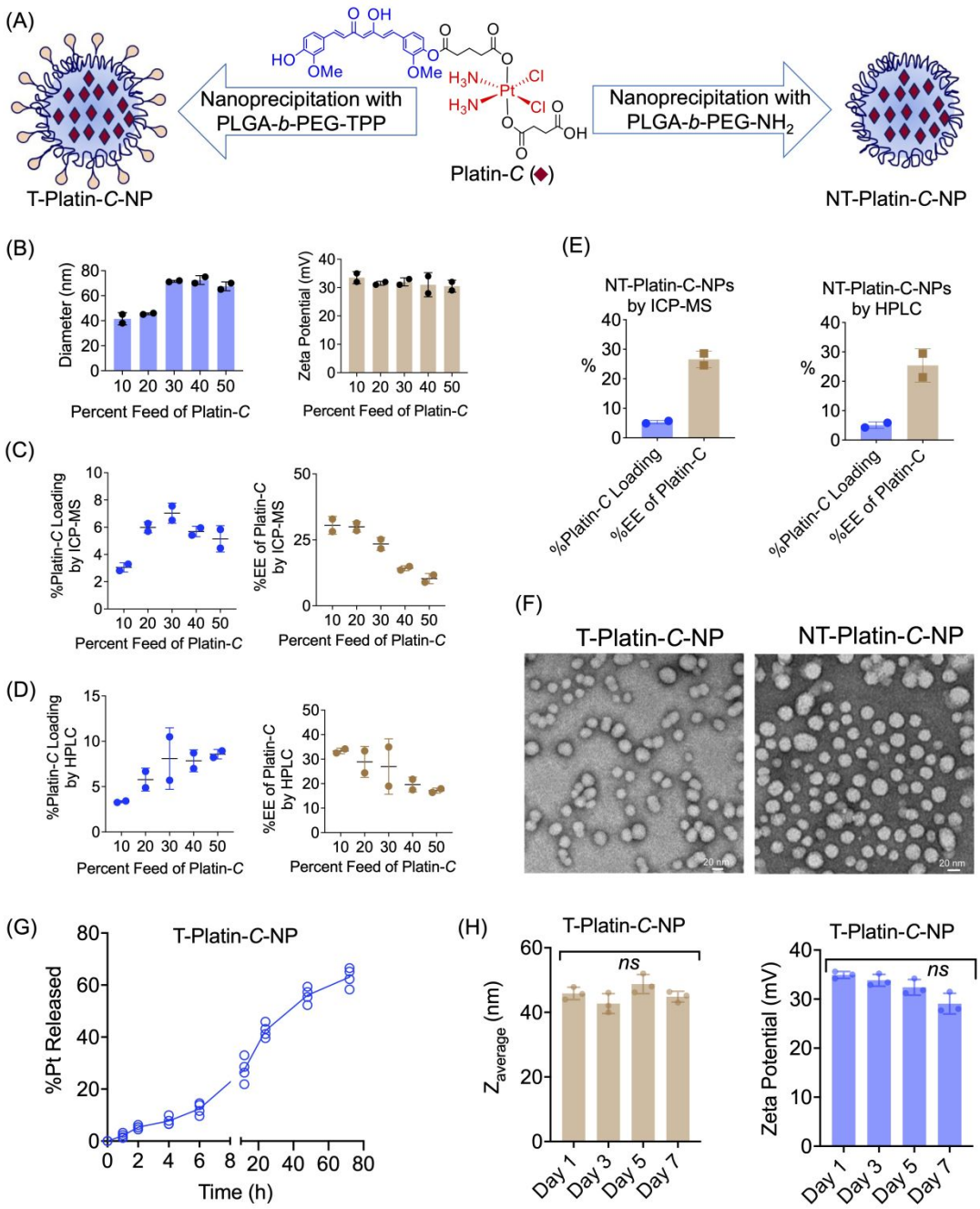

Fig. 2. (A) Schematic representation of the synthesized nanoparticles. (B) Hydrodynamic diameter and zeta potential of T-Platin-*C*-NPs containing various feeds of Platin-C, as determined by Dynamic Light Scattering (DLS) measurements. Comparison of percent loading (%L) and percent encapsulation efficiency (%EE) for a batch of T-Platin-*C*-NPs, whose hydrodynamic diameter (diameter, in nm) and zeta potential (in mV) are depicted in (B), as determined by (C) ICP-MS and (D) HPLC techniques. (E) Comparison of percent loading (%L) and %EE for a batch of NT-Platin-*C*-NPs at a 20% feed of Platin-C by ICP-MS and HPLC techniques. (F) Transmission electron microscopy (TEM) images of T-Platin-*C*-NPs and NT-Platin-*C*-NPs. (G) Release kinetics study of Platin-*C* from T-Platin-*C*-NPs. (H) Stability of T-Platin-*C*-NPs as determined by DLS measurements.

Time dependent release study of the prodrug was performed by dialyzing the T-Platin-*C*-NPs against 1X PBS at physiologically relevant pH of 7.4 (Fig. 2G). It is evident that the NPs exhibit a controlled release profile as seen from the gradual release of Platin-*C* and it took 80 h to achieve a release of ~70%. Stability studies conducted for 7 days demonstrated that there was no abrupt change in size and zeta potential of the NPs as measured by DLS (Fig. 2H). So, NPs prepared for all the subsequent studies were used within a week of their synthesis. As we moved further with the studies as described below, we were able to show that the cisplatin-curcumin combination therapeutic agent, Platin-*C*, was cytotoxic towards cisplatin resistant A2780/CP70 cells (Scheme 1). Moreover, it was successfully delivered preferentially into the mitochondria of these cells as observed using confocal microscopy and the toxicity of the nanoformulation enhanced by almost 4-folds as compared to the free Platin-*C*.

Cellular cytotoxicity in A2780/CP70 cells

Our primary objective in developing Platin-*C* is to enhance the cytotoxic potential of platinum drugs. In addition, we also aimed at modifying cisplatin in a manner so as to overcome resistance attained by certain cancer cell types. So, we chose to evaluate cell-kill activity of Platin-*C* in cisplatin resistant human ovarian cancer cell line A2780/CP70. The results of this experiment appeared to be encouraging. With IC_{50} value of ~26 μM, Platin-*C* was found to be much less cytotoxic than either cisplatin or curcumin. While cisplatin showed an IC_{50} value of ~12 μM, that of curcumin was ~9 μM. When the cells were presented with a mixture of both cisplatin and curcumin, the IC_{50} value dropped further to ~8 μM. Nevertheless, toxicity of Platin-*C* improved greatly when it was packaged into the polymeric nanoformulations. The IC_{50} value for NT-Platin-*C*-NP was ~11 μM whereas that for the T-Platin-*C*-NP was ~5 μM. This could be due to the enhancement in cellular uptake of the complex facilitated by nano-encapsulation. Furthermore, this observation reiterates the importance of drug accumulation inside mitochondria of cells for the achievement of maximum toxicity. Higher toxicity of the targeted nanoparticles in comparison to the non-targeted ones could be attributed to the successful delivery of Platin-*C* into the mitochondria of cells utilizing the lipophilic positive charge on the TPP cation. Also, cisplatin being one of the reduction products of Platin-*C*, upon accumulation inside the cellular mitochondrion might have easier access to mitochondrial DNA (mt-DNA) thereby trigger cell death *via* mt-DNA damage.[54] On the other hand, despite the positive surface charge on the NT-Platin-*C*-NPs, the absence of lipophilic character and effective charge delocalization on the amine terminus might have rendered them incapable of targeting mitochondria efficiently. A comparison of the IC_{50} values have been presented in the Fig. 3 and the representative MTT assay plots have been presented in Supp. Fig. 14.

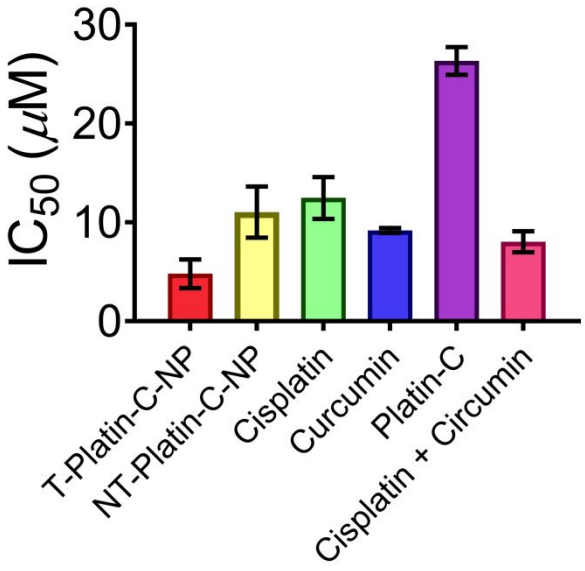

	IC_{50} (μM)
T-Platin-C-NP	4.8 ± 1.2
NT-Platin-C-NP	11.0 ± 1.1
Cisplatin	12.5 ± 1.1
Curcumin	9.2 ± 1.5
Platin-C	26.3 ± 2.1
Cisplatin + Curcumin	8.1 ± 1.8

Fig. 3. Comparison of the IC_{50} values of Platin-*C*-NPs and all the relevant controls on A2780/CP70 cells as determined by MTT assay. The drug candidates alone (*viz.* Cisplatin, Curcumin or Platin-*C*) or as physical mixtures (*viz.,* Cisplatin + Curcumin) were used as control test articles.

Mitochondrial colocalization of Platin-*C* in A2780/CP70 cells

To ascertain the mitochondria targeting capabilities of the nanoparticles, we performed confocal microscopy experiments on A2780/CP70 cells incubated with the nanoparticles (Fig. 4). To our advantage, the green fluorescence of curcumin ligand enabled monitoring of intracellular localization pattern of Platin-*C* NPs. DAPI containing stain NucBlue® was used to stain the nucleus and MitoTracker® Red FM was used to stain the mitochondria of cells. We found that both the nanoparticles were internalized into the cells as evidenced from the green fluorescence inside cells. Therefore, both the nanoparticle formulations exhibit enhancement in cytotoxic potential of Platin-*C* upon encapsulation as evidenced from the IC_{50} values mentioned above. Both targeted and non-targeted nanoparticles localized primarily in the cytosol but the extent of colocalization of the T-Platin-*C*-NP with the mitochondria was greater than that of the NT-Platin-*C*-NP. This was confirmed by determining the Pearson correlation coefficients, 0.84 and 0.46 for the targeted and non-targeted NP samples respectively. This observation confirms our hypothesis that the TPP containing T-Platin-*C*-NPs were able to target mitochondria more efficiently than the NT-Platin-*C*-NPs.

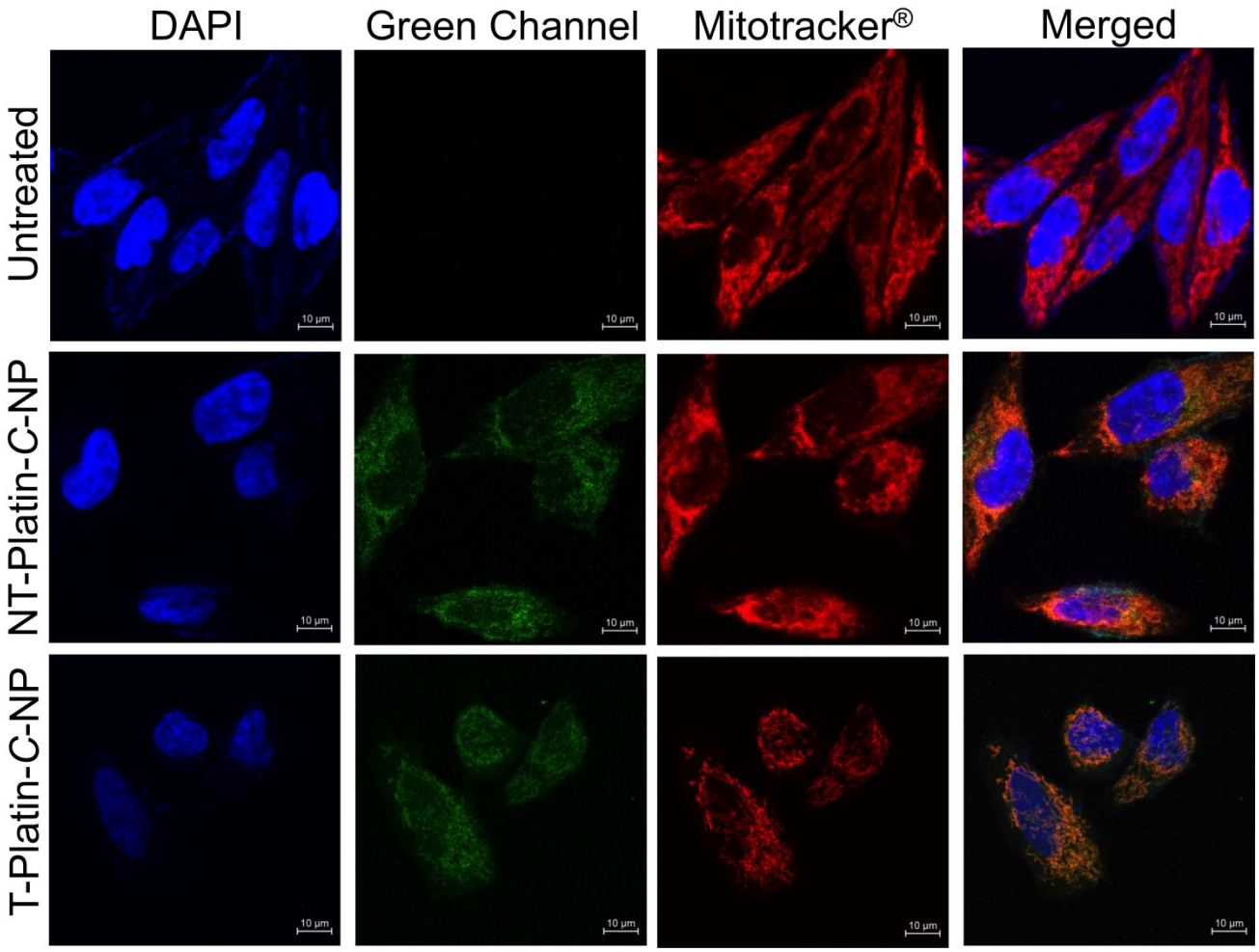

Fig. 4. Cellular localization of targeted and non-targeted Platin-*C*-NPs in A2780/CP70 cells visualized using confocal laser scanning microcope showing significantly enhanced co-localization of the targeted Platin-C nanoconstructs with the michondrial stain, Mitotracker®-Red.

Mitochondrial Activity of T-Platin-*C*-NP

The design of our targeted polymeric nano-platforms for delivery of Platin-*C* was based on the premise that the drug payload gets preferentially delivered to mitochondria. NT-Platin-*C*-NPs were designed to serve as appropriate controls. To determine the effect of these Platin-*C* loaded nanoparticles on the health of mitochondria in cancer cells, we had performed mitostress test on A2780 (Fig. 5A) and A2780/CP70 (Fig. 5B) cells treated with the NP constructs. Mitostress test monitors the oxygen consumption rate (OCR) of the cells under the influence of oligomycin, FCCP, antimycin-A and rotenone and thereby provides a measure of the mitochondrial respiration of these treated cells. A stark difference was observed between the mitochondrial behavior of the cisplatin sensitive A2780 cells and cisplatin resistant A2780/CP70 cells. While both the targeted and non-targeted NPs were equally effective in inhibiting the mitochondrial performance of both the cell lines, the targeted construct was found to be more effective in the cisplatin resistant cells. This pattern becomes more evident from the basal respiration and ATP production levels of the two treated cell lines. This could be indicative of the fact that in A2780 cells Platin-*C* induces cell death *via* damage to both genomic and mitochondrial DNA while in A2780/CP70 cells, where genomic DNA is resistant to damage induced by platinum

drugs, the T-Platin-*C*-NPs effects cells death by inflicting damage preferentially to the mitochondrial DNA.

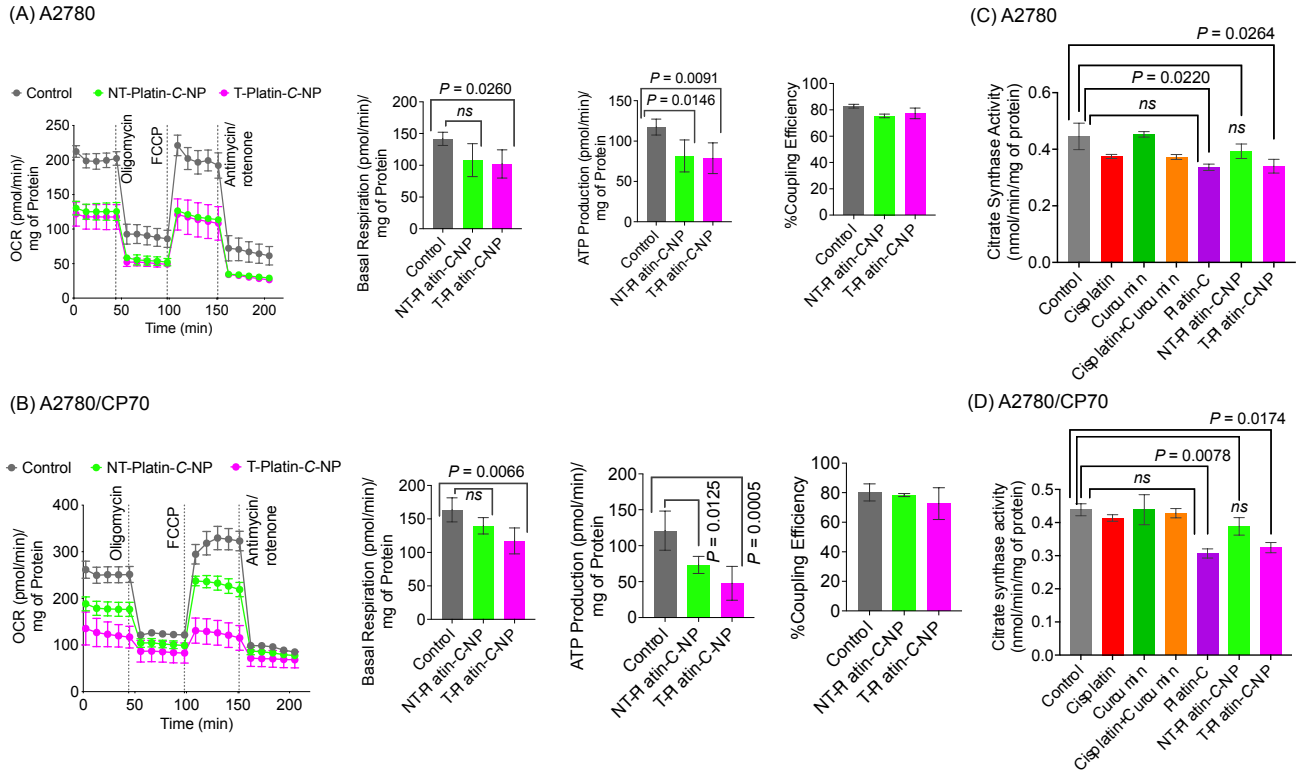

Fig. 5. Assessment of the impact of the nanoconstructs, free Platin-C, curcumin and cisplatin on the overall mitochondrial health of cancer cells by Mitostress test in (A) A2780 cells and (B) A2780/CP70 cells, and Citrate Synthase Activity assay in (C) A2780 cells and (D) A2780/CP70 cells. Statistical analyses were performed using ordinary one way ANOVA.

To further ascertain the effect of the T-Platin-*C*-NPs on cellular mitochondria, we performed citrate synthase activity assay. Citrate synthase is a mitochondrial enzyme and its activity is often used as a marker for functionally active mitochondria and mitochondrial content.[57] In both A2780 (Fig. 5C) and A2780/CP70 (Fig. 5D) cells, treatment with T-Platin-*C*-NPs demonstrated significant diminished levels of citrate synthase activity compared to the non-targeted NPs, curcumin, cisplatin or their physical mixture. It must also be noted that the citrate synthase activity was affected by Platin-*C* to comparable levels as that of the targeted nanoparticles. This could mean that the mitochondria directed activity of the targeted nanoformulation is primarily because of the Platin-*C* prodrug. It is just that the targeted construct is able to direct it to the mitochondria while the non-targeted ones cannot.

Curbing tumor-associated inflammation in cells using Platin-*C*

Inflammation is intricately associated with tumor development and progression.[11] Also, chemotherapeutic agents are known to generate inflammatory response and are therefore responsible for unwanted side effects.[43] Platin-*C* was designed as a combination therapeutic agent that could simultaneously deliver a chemotherapeutic agent, cisplatin and an anti-inflammatory agent , curcumin. We set out to explore the anti-inflammatory activity of Platin-*C* and its NPs using Western Blotting and real-time polymerase chain reaction (RT-PCR) techniques in PC-3 cells (Fig. 6). Bacterial lipopolysaccharides (LPS) engage toll-like receptors (TLRs) to induce immune responses and such

TLR agonists have been shown to stimulate PC-3 cells towards generation of pro-inflammatory cytokines and chemokines.[58] We used bacterial LPS to induce inflammatory pathways in these cells. Western Blot analyses evidenced up regulation of TNF-α and NF-κB in these cells and T-Platin-*C*-NP treatment was able to reduce the elevated levels of these markers more efficiently compared to NT-Platin-*C*-NP (Fig. 6A). Quantification of the protein levels further supported the conclusion (Fig. 6B). RT-PCR analyses of mRNA expression of these markers indicated that both targeted and non-targeted nanoparticles loaded with Platin-*C* were able to diminish the levels of pro-inflammatory cytokines, IL-6 and TNF-α and down-regulate NF-κB and superoxide dismutase-2 (SOD-2) in LPS treated PC-3 cells (Fig. 6C). While NF-κB acts as a key regulator of tumor associated inflammation, such inflammation is also known to elicit SOD-2 upregulation.[59] Among the reduction products of Platin-*C*, cisplatin is incapable of exhibiting any anti-inflammatory activity as reported earlier.[43] Therefore the anti-inflammatory activity of Platin-*C* could be attributed to the curcumin conjugate.

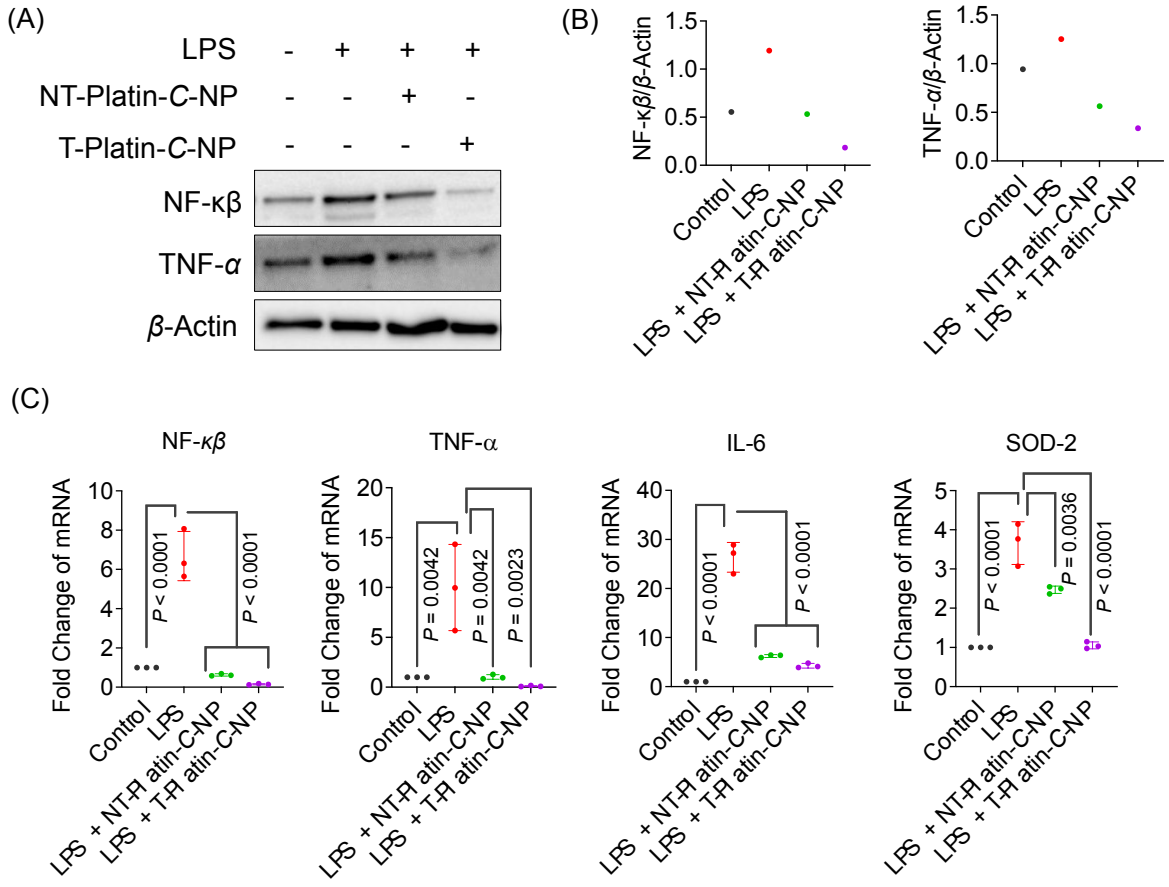

Fig. 6. (A) Western Blot images and (B) desitometric analyses of the respective bands for NF-$\kappa\beta$ and TNF-α with respect to β-Actin. (C) RT-PCR results expressed as fold change of mRNA expression corresponding to NF-$\kappa\beta$, TNF-α, IL-6 and SOD-2 with respect to β-Actin. Statistical analyses were performed using ordinary one way ANOVA.

Conclusion

This work aimed at designing a Pt(IV)-based combination therapeutic agent and deliver it using suitably decorated polymeric nanoparticle for site-selective delivery and action. In our attempt we have been successful in synthesizing Platin-*C* by combining cisplatin and curcumin into a Pt(IV) coordination complex. The synthesis of this complex involved multiple step modification of cisplatin and curcumin, which were finally assembled into Platin-*C*. Positively charged nanoparticle platforms were also developed by suitably modifying PLGA-*b*-PEG polymers bearing NH_2 and TPP terminus. Purity of Platin-*C* polymers and the corresponding were ascertained employing suitable characterization techniques. It was found that the nanoparticles were capable of encapsulating Platin-*C* efficiently into positively charged spherical nanoparticles with uniform sizes and shapes. The nanoparticles were able to deliver the encapsulated complex inside cells and the T-Platin-*C*-NP showed enhanced selectivity towards the mitochondria of A2780/CP70 cells. The design of the complex together with the site-selectivity offered by the NPs rendered these nano-constructs with great potential towards eliciting cytotoxicity in these cisplatin-resistant cells. Our observations further emphasized the fact that mere positive charge on nanoparticle surface may not be enough to evoke mitochondria-targeting property unless it is protected inside a hydrophobic environment as is the case with triphenylphosphonium (TPP) cation. Our findings show that Platin-*C* is capable of inducing mitochondria-directed toxicity as evident from its effect on mitochondrial respiration pattern and inhibition of mitochondrial enzymes, more so, when it is packaged in mitochondria-targeted polymeric nanoparticles. Finally, we were also able to establish that in addition to exhibiting mitochondria directed anti-cancer activity in cisplatin-resistant cells, Platin-*C* is capable of tackling associated inflammatory characteristics.

Conflict of Interest

The authors declare that the research was conducted in the absence of any commercial or financial relationships that could be construed as a potential conflict of interest.

Author Contributions

S.D. and B.B. conceived the idea. S.D. provided resources and supervised the research. B.B., A.A., J.H.C., and B.S. performed the experiments. B.B., A.A., J.H.C., B.S., and S.D. analysed the data. B.B. and S.D. wrote the manuscript. All authors approved the final version of the manuscript.

Funding

This work was supported by Department of Defense Prostate Cancer Idea Award (W81XWH-12-1-0406) to S.D. We also thank Sylvester Comprehensive Cancer Center and Florida Department of Health Bankhead Coley Cancer Research Award (8BC10) for financial support. BB acknowledges DST-INSPIRE Faculty award (DST/INSPIRE/04/2017/001644; Faculty Registration No. IFA17-CH258) from Department of Science and Technology (DST), India.

Acknowledgments

We thank the Biomedical Microscopy Core at University of Georgia for confocal microscope facility.

References

(1) Ghosh, S. *Bioorganic Chemistry* **2019**, *88*, 102925.

(2) Wilson, J. J.; Lippard, S. J. *Chemical Reviews* **2014**, *114*, 4470.

(3) Basu, U.; Banik, B.; Wen, R.; Pathak, R. K.; Dhar, S. *Dalton Transactions* **2016**, *45*, 12992.

(4) Dasari, S.; Tchounwou, P. B. *Eur J Pharmacol* **2014**, *740*, 364.

(5) Makovec, T. *Radiol Oncol* **2019**, *53*, 148.

(6) Achkar, I. W.; Abdulrahman, N.; Al-Sulaiti, H.; Joseph, J. M.; Uddin, S.; Mraiche, F. *Journal of Translational Medicine* **2018**, *16*, 96.

(7) Wheate, N. J.; Walker, S.; Craig, G. E.; Oun, R. *Dalton transactions (Cambridge, England : 2003)* **2010**, *39*, 8113.

(8) Grivennikov, S. I.; Greten, F. R.; Karin, M. *Cell* **2010**, *140*, 883.

(9) Greten, F. R.; Grivennikov, S. I. *Immunity* **2019**, *51*, 27.

(10) Singh, N.; Baby, D.; Rajguru, J. P.; Patil, P. B.; Thakkannavar, S. S.; Pujari, V. B. *Ann Afr Med* **2019**, *18*, 121.

(11) Zhao, H.; Wu, L.; Yan, G.; Chen, Y.; Zhou, M.; Wu, Y.; Li, Y. *Signal Transduction and Targeted Therapy* **2021**, *6*, 263.

(12) Hoesel, B.; Schmid, J. A. *Mol Cancer* **2013**, *12*, 86.

(13) Yang, C. H.; Murti, A.; Pfeffer, S. R.; Basu, L.; Kim, J. G.; Pfeffer, L. M. *Proceedings of the National Academy of Sciences* **2000**, *97*, 13631.

(14) Chen, F.; Castranova, V.; Shi, X. *Am J Pathol* **2001**, *159*, 387.

(15) Guttridge, D. C.; Albanese, C.; Reuther, J. Y.; Pestell, R. G.; Baldwin, A. S. *Molecular and Cellular Biology* **1999**, *19*, 5785.

(16) Akbari, E.; Akhavan, O.; Hatamie, S.; Rahighi, R. *Journal of Drug Delivery Science and Technology* **2018**, *45*, 422.

(17) Mukerjee, A.; Sørensen, T. J.; Ranjan, A. P.; Raut, S.; Gryczynski, I.; Vishwanatha, J. K.; Gryczynski, Z. *The Journal of Physical Chemistry B* **2010**, *114*, 12679.

(18) Nardo, L.; Andreoni, A.; Masson, M.; Haukvik, T.; Tønnesen, H. H. *Journal of Fluorescence* **2011**, *21*, 627.

(19) Tomeh, M. A.; Hadianamrei, R.; Zhao, X. *Int J Mol Sci* **2019**, *20*, 1033.

(20) Wilken, R.; Veena, M. S.; Wang, M. B.; Srivatsan, E. S. *Mol Cancer* **2011**, *10*, 12.

(21) Gupta, A. P.; Khan, S.; Manzoor, M. M.; Yadav, A. K.; Sharma, G.; Anand, R.; Gupta, S. In *Studies in Natural Products Chemistry*; Atta ur, R., Ed.; Elsevier: 2017; Vol. 54, p 355.

(22) Menon, V. P.; Sudheer, A. R. *Advances in experimental medicine and biology* **2007**, *595*, 105.

(23) Hewlings, S. J.; Kalman, D. S. *Foods* **2017**, *6*, 92.

(24) Fadus, M. C.; Lau, C.; Bikhchandani, J.; Lynch, H. T. *Journal of Traditional and Complementary Medicine* **2017**, *7*, 339.

(25) Alisi, I. O.; Uzairu, A.; Abechi, S. E.; Idris, S. O. *Journal of Advanced Research* **2018**, *12*, 47.

(26) Menon, V. P.; Sudheer, A. R. In *The Molecular Targets and Therapeutic Uses of Curcumin in Health and Disease*; Aggarwal, B. B., Surh, Y.-J., Shishodia, S., Eds.; Springer US: Boston, MA, 2007, p 105.

(27) van't Land, B.; Blijlevens, N. M. A.; Marteijn, J.; Timal, S.; Donnelly, J. P.; de Witte, T. J. M.; M'Rabet, L. *Leukemia* **2004**, *18*, 276.

(28) Marquardt, J. U.; Gomez-Quiroz, L.; Arreguin Camacho, L. O.; Pinna, F.; Lee, Y.-H.; Kitade, M.; Domínguez, M. P.; Castven, D.; Breuhahn, K.; Conner, E. A.; Galle, P. R.; Andersen, J. B.; Factor, V. M.; Thorgeirsson, S. S. *J Hepatol* **2015**, *63*, 661.

(29) Jovanovic, S. V.; Steenken, S.; Boone, C. W.; Simic, M. G. *Journal of the American Chemical Society* **1999**, *121*, 9677.

(30) Siviero, A.; Gallo, E.; Maggini, V.; Gori, L.; Mugelli, A.; Firenzuoli, F.; Vannacci, A. *Journal of Herbal Medicine* **2015**, *5*, 57.

(31) Anand, P.; Kunnumakkara, A. B.; Newman, R. A.; Aggarwal, B. B. *Molecular Pharmaceutics* **2007**, *4*, 807.

(32) Bansal, S. S.; Goel, M.; Aqil, F.; Vadhanam, M. V.; Gupta, R. C. *Cancer Prev Res (Phila)* **2011**, *4*, 1158.

(33) Mirzaie, Z.; Barati, M.; Tokmedash, M. A. *Pharmaceutical Chemistry Journal* **2020**, *54*, 353.

(34) Mitra, K.; Gautam, S.; Kondaiah, P.; Chakravarty, A. R. *Angew Chem Int Ed Engl* **2015**, *54*, 13989.

(35) Upadhyay, A.; Gautam, S.; Ramu, V.; Kondaiah, P.; Chakravarty, A. R. *Dalton Transactions* **2019**, *48*, 17556.

(36) Mitra, K.; Gautam, S.; Kondaiah, P.; Chakravarty, A. R. *European Journal of Inorganic Chemistry* **2017**, *2017*, 1753.

(37) Banerjee, S.; Chakravarty, A. R. *Accounts of Chemical Research* **2015**, *48*, 2075.

(38) Wanninger, S.; Lorenz, V.; Subhan, A.; Edelmann, F. T. *Chemical Society Reviews* **2015**, *44*, 4986.

(39) Sarkar, T.; Banerjee, S.; Hussain, A. *RSC Advances* **2015**, *5*, 16641.

(40) Renfrew, A. K.; Bryce, N. S.; Hambley, T. *Chemistry – A European Journal* **2015**, *21*, 15224.

(41) Garai, A.; Pant, I.; Banerjee, S.; Banik, B.; Kondaiah, P.; Chakravarty, A. R. *Inorganic Chemistry* **2016**, *55*, 6027.

(42) Banik, B.; Somyajit, K.; Nagaraju, G.; Chakravarty, A. R. *Dalton Transactions* **2014**, *43*, 13358.

(43) Pathak, R. K.; Marrache, S.; Choi, J. H.; Berding, T. B.; Dhar, S. *Angewandte Chemie International Edition* **2014**, *53*, 1963.

(44) Pathak, R. K.; Basu, U.; Ahmad, A.; Sarkar, S.; Kumar, A.; Surnar, B.; Ansari, S.; Wilczek, K.; Ivan, M. E.; Marples, B.; Kolishetti, N.; Dhar, S. *Biomaterials* **2018**, *187*, 117.

(45) Surnar, B.; Kolishetti, N.; Basu, U.; Ahmad, A.; Goka, E.; Marples, B.; Kolb, D.; Lippman, M. E.; Dhar, S. *Biochemistry* **2018**, *57*, 6500.

(46) Kianamiri, S.; Dinari, A.; Sadeghizadeh, M.; Rezaei, M.; Daraei, B.; Bahsoun, N. E.; Nomani, A. **2020**, *17*, 4483.

(47) Gao, C.; Wang, Y.; Sun, J.; Han, Y.; Gong, W.; Li, Y.; Feng, Y.; Wang, H.; Yang, M.; Li, Z.; Yang, Y.; Gao, C. *Acta Biomater* **2020**, *108*, 285.

(48) Reddy, C. A.; Somepalli, V.; Golakoti, T.; Kanugula, A. K.; Karnewar, S.; Rajendiran, K.; Vasagiri, N.; Prabhakar, S.; Kuppusamy, P.; Kotamraju, S.; Kutala, V. K. *PLOS ONE* **2014**, *9*, e89351.

(49) Wen, R.; Banik, B.; Pathak, R. K.; Kumar, A.; Kolishetti, N.; Dhar, S. *Advanced Drug Delivery Reviews* **2016**, *99*, 52.

(50) Murphy, M. P. *Biochimica et Biophysica Acta (BBA) - Bioenergetics* **2008**, *1777*, 1028.

(51) Murphy, M. P. *Trends in Biotechnology* **1997**, *15*, 326.

(52) Smith, R. A. J.; Porteous, C. M.; Gane, A. M.; Murphy, M. P. *Proceedings of the National Academy of Sciences* **2003**, *100*, 5407.

(53) Marrache, S.; Dhar, S. *Proceedings of the National Academy of Sciences* **2012**, *109*, 16288.

(54) Marrache, S.; Pathak, R. K.; Dhar, S. *Proceedings of the National Academy of Sciences* **2014**, *111*, 10444.

(55) Kalathil, A. A.; Kumar, A.; Banik, B.; Ruiter, T. A.; Pathak, R. K.; Dhar, S. *Chem Commun (Camb)* **2016**, *52*, 140.

(56) Pathak, R. K.; Dhar, S. *Journal of the American Chemical Society* **2015**, *137*, 8324.

(57) Banik, B.; Askins, B. W.; Dhar, S. *Nanoscale* **2016**, *8*, 19581.

(58) Mukherjee, S.; Siddiqui, M. A.; Dayal, S.; Ayoub, Y. Z.; Malathi, K. *Journal of inflammation research* **2014**, *7*, 89.

(59) Yi, L.; Shen, H.; Zhao, M.; Shao, P.; Liu, C.; Cui, J.; Wang, J.; Wang, C.; Guo, N.; Kang, L.; Lv, P.; Xing, L.; Zhang, X. *Scientific reports* **2017**, *7*, 7953.